A Simple Approach for Improving Bandwidth and Isolation of Wilkinson Power Divider

Nguyen Minh GIANG, Luong Duy MANH

Dept. of Radioelectronic Engineering, Le Quy Don Technical University, Hoang Quoc Viet Street 236, Hanoi, Vietnam

manhld@lqdtu.edu.vn

Submitted November 24, 2021 / Accepted April 23, 2022

Abstract. *A simple approach to improve both the bandwidth and isolation of the Wilkinson power divider for using in L-band satellite communications is presented in this paper. To enhance the bandwidth, a multi-section method based on the Chebychev impedance transformation is employed. In order to improve the isolation performance between output ports, the values of isolation resistors are carefully determined by using the iterative approximation method combined with an investigation procedure. In order to validate the proposed design, a two-way and eight-way power divider prototypes were fabricated and tested on a Rogers RO4003C material. Good agreements between simulations and measurements are obtained in a frequency range from 0.8 GHz to 2.2 GHz. The two-way power divider had a fractional bandwidth of 106% with an isolation of better than 30 dB. The eight-way power divider achieved the bandwidth and isolation of 109% and better than 24 dB, respectively. Both the power dividers exhibit the phase imbalance of less than 3 degrees, and amplitude imbalance of less than 0.02 dB. Compared with the other works, the proposed power dividers deliver broader bandwidth and improved isolation while still retaining good insertion loss, low phase and amplitude imbalance in the operation frequency range.*

Keywords

Wilkinson power divider, high isolation, wideband PD, Chebyshev impedance transformation, satellite communication

1. Introduction

Wilkinson power divider (PD) is commonly used in a variety of important applications such as frequency mixing circuits, power amplifiers, phased array antenna, and satellite communication because of its promising advantages including low insertion loss and high isolation [1], [2]. However, conventional Wilkinson PD exhibits a narrow bandwidth, making it difficult to be used in broadband communication systems. Different modified PD structures have been proposed to expand the bandwidth. In [3], a wideband PD is designed employing defected ground structures [3]. In [4], a PD of high selectivity using four pairs of coupled lines loaded with a T-shaped stub has been proposed. A power divider with ultra-broadband based on tapered lines is designed in [5]. In these works, although the bandwidth can be improved, the isolation is not improved simultaneously. In addition, the isolation performance presented in [3], [4] is only 20 dB while this level in [5] is 15 dB. In [6], an ultra-wideband Wilkinson power divider is fabricated using a hermetic multi-wafer level packaging technology. It allows to expand the bandwidth and reduce the size of the circuit. However, the disadvantage of this circuit is that it has a high insertion loss of more than 1 dB and high amplitude imbalance of 0.4 dB as well as a high phase imbalance of higher than 3°.

Numerous techniques have been introduced in an attempt to improve the isolation of PDs, such as using distributed isolation to replace the conventional resistor isolation network [7], using an 'RLCT' isolation network [8], employing multistage isolation [9], and by introducing a highly symmetric coupling structure of the divider [10]. However, these methods are not capable of improving the bandwidth simultaneously. The isolation level achieved in [7] is better than 23 dB, but the bandwidth is only 56.6%. In [8], the PD has wider bandwidth at a level of 61% with a minimum isolation of 20 dB. However, the insertion loss of 1 dB is relatively high. The PD presented in [9] achieves a wide bandwidth and an insertion loss of 0.3 dB, but the isolation level is just 20 dB. The PD in [10] gives an isolation of better than 30 dB, but it exhibits a narrow bandwidth of 3.5% with a high insertion loss of 1.4 dB and a high amplitude imbalance from 0.22 to 0.65 dB.

In this paper, we propose a simple approach to simultaneously improve the bandwidth and isolation of the Wilkinson PD while still retaining the remaining performance such as insertion loss, phase and amplitude imbalances. Two-way and eight-way PDs were designed, fabricated, and tested to verify the proposed approach.

2. Proposed Approach

The traditional Wilkinson PD is composed of quarter-wavelength microstrip lines to match impedances between

DOI: 10.13164/re.2022.0224

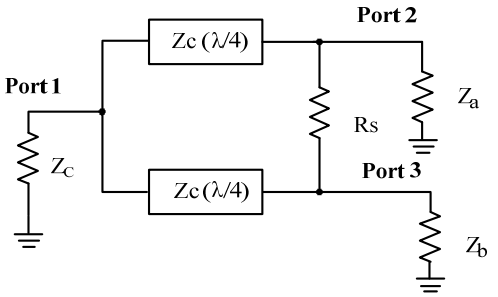

Fig. 1. Conventional Wilkinson power divider.

input and output ports as shown in Fig. 1.

To improve the isolation performance, an isolation resistor R_S is added between two branches of the circuit, the values of Z_C and R_S are determined by the expressions:

$$Z_c = \sqrt{2Z_a Z_b}\,, \tag{1}$$

$$R_s = 2Z_b\,. \tag{2}$$

The traditional Wilkinson PD exhibits an inherent narrow bandwidth. In order to extend the bandwidth of this circuit, multi-section impedance transformation technique is applied in this work. According to this technique, multiple segments are used instead of using one microstrip line to match load and transmission line impedances. According to the small reflection theory (TSR) [11], the reflection coefficient of the circuit including N segments with the same electrical length θ can be defined by the reflection coefficients of each segment. Therefore, by selecting appropriate number of segments N and reflection coefficients of each segment, we can obtain the desired reflection coefficient of the entire circuit $\Gamma(\theta)$. In order to approximate response function of the circuit, the Chebyshev function is employed. According to [11], fractional bandwidth (FBW) of the transmission line can be calculated using (3):

$$\frac{\Delta f}{f_0} = 2 - \frac{4\theta_m}{\pi} \tag{3}$$

where f_0 is the central frequency and θ_m is the corner electrical length at the maximum allowed magnitude of $\Gamma(\theta)$ in the passband and is given as:

$$\sec\theta_m = \cosh\left[\frac{1}{N}\cosh^{-1}\left(\frac{\ln\left(Z_L/Z_0\right)}{2\Gamma_m}\right)\right] \tag{4}$$

where Z_L and Z_0 are load and source impedances, respectively, Γ_m is the maximum value of reflection coefficient that can be tolerated over the passband.

From (3) and (4), it can be seen that the number of sections N can be calculated for given FBW and Γ_m. In this work, Γ_m and FBW are chosen to be 0.015 and 93.3%, respectively. Hence, N is calculated to be 4. The structure of the PD is then constructed as shown in Fig. 2. It consists of four quarter-wavelength transmission line sections having corresponding characteristic impedances Z_1, Z_2, Z_3 and Z_4. Here R_1, R_2, R_3, and R_4 are the isolation resistors.

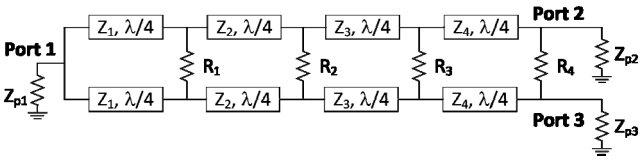

Fig. 2. Block diagram of the proposed two-way power divider.

Section No.	Calculated impedance (Ω)
Z_1	92.8
Z_2	78.6
Z_3	63.6
Z_4	53.8

Tab. 1. Calculated impedance values of the four sections.

The impedances are calculated using the corresponding reflection coefficient at each section based on the TSR by the following equations:

$$\theta_m = \left(2 - \frac{\Delta f}{f_0}\right)\frac{\pi}{4}, \tag{5}$$

$$\Gamma_0 = \frac{\Gamma_m \cdot \sec^4\theta_m}{2}, \tag{6}$$

$$\Gamma_1 = 2\Gamma_m\left(\sec^4\theta_m - \sec^2\theta_m\right), \tag{7}$$

$$\Gamma_2 = \Gamma_m\left(3\sec^4\theta_m - 4\sec^2\theta_m + 1\right), \tag{8}$$

$$\Gamma_3 = \Gamma_1, \tag{10}$$

$$Z_{n+1} = Z_n\, e^{2\Gamma_n}\,. \tag{11}$$

The calculated results are shown in Tab. 1.

It is well known that the isolation performance of the PD depends mainly on the isolation resistors R_1–R_4. These resistors can be calculated by the iterative approximation method [12]. Although this method can improve the isolation, the best isolation is usually limited at a level of 20 dB. In order to further improve the isolation performance, the method needs being modified. The proposed modified method for calculating isolation resistors consists of two steps: the first step is preliminary calculation of the isolation resistors by the iterative approximation method. The second one is optimizing the isolation resistor values by using an investigation method. In the first step, the initially calculated values of the isolation resistors are: $R_1 = 106\ \Omega$, $R_2 = 155\ \Omega$, $R_3 = 281\ \Omega$, $R_4 = 708\ \Omega$. In the first step, the value of R_4 is first calculated, and the remaining resistors are then determined depending on the value of R_4. Therefore, the variation of the isolation between the output ports on the change of R_4 can be investigated. By this way, the values of isolation resistors can be optimized to achieve high isolation performance. This investigation is carried out in the second step. Figure 3 shows the dependence of the isolation between two output ports of the PD on the variation of R_4.

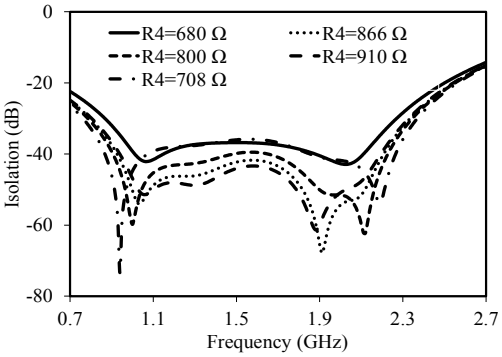

Fig. 3. Dependence of the isolation performance on the variation of R_4.

From Fig. 3, it is clear that R_4 = 866 Ω gives the best isolation performance in the operation frequency range. The values of the remaining resistors are then re-calculated as follows: R_1 = 123 Ω, R_2 = 198 Ω, R_3 = 324 Ω.

3. Simulation and Measurement of the Proposed Two-way Power Divider

Based on the proposed design procedure, a two-way PD was designed, fabricated and tested. Figure 4 shows the fabricated prototype of PD. The material used is Rogers RO4003C with a substrate thickness of 22-mil and 1-oz copper thickness. The total area of PD is 5.0 cm × 5.0 cm. The dimensions of the four sections of the PD circuit are tabulated in Tab. 2.

The ADS 2019 simulator is employed to make simulations and a Vector Network Analyzer PNA-X N5242A from Keysight is used to measure performance of the fabricated PD. The experimental setup is described in Fig. 5. The simulated and measured results of isolation between two output ports of the PD are shown in Fig. 6.

Section No.	Dimension (mm)	
	Width	Length
Z_1	0.46	31.20
Z_2	0.69	30.79
Z_3	1.10	30.27
Z_4	1.44	29.89

Tab. 2. Calculated dimension of four sections.

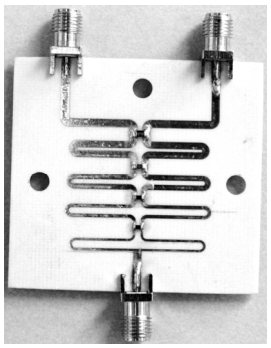

Fig. 4. Fabricated two-way power divider.

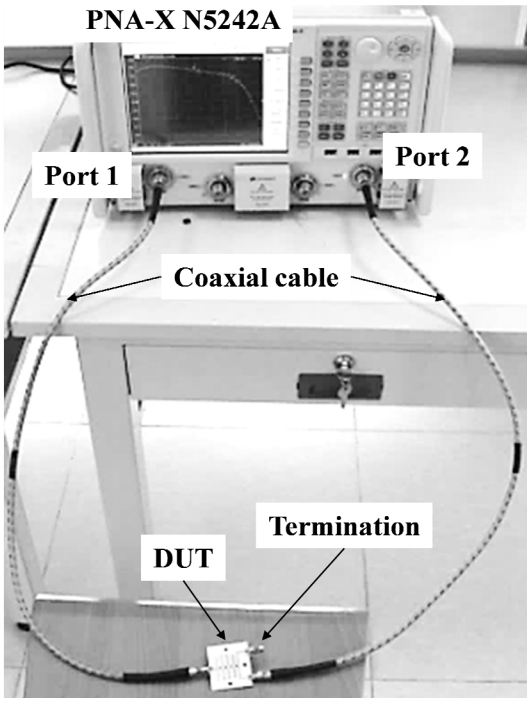

Fig. 5. Experimental setup.

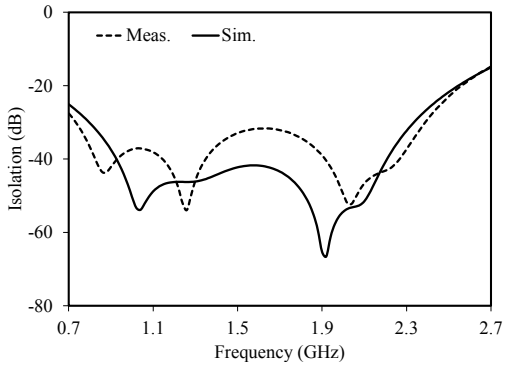

Fig. 6. Simulation (Sim.) and measured (Meas.) isolation of the two-way PD prototype.

As can be seen in Fig. 6, simulated results agree well with the measured ones. Particularly, in the operation frequency range from 0.7 to 2.4 GHz, the measured isolation is better than 30 dB.

Figure 7 shows the simulated and measured insertion loss of the proposed power divider. It is clearly seen that the measured results are highly consistent with the simulated one. The measured insertion loss varies from 0.2 to 0.5 dB over the frequency range from 0.7 to 2.4 GHz with a fractional bandwidth of 106%.

After isolation and insertion loss have been both improved, the amplitude and phase imbalance will be validated. The difference between two outputs, namely amplitude imbalance (*AI*), is calculated by the formula:

$$AI = \left| S(2,1) - S(3,1) \right| \tag{12}$$

where $S(2,1)$ and $S(3,1)$ are S-parameters of the PD. The measured amplitude imbalance of the proposed PD is

shown in Fig. 8. As can be seen from Fig. 8, within the passband, the measured amplitude imbalance of PD is less than 0.12 dB.

Simulated and measured phase imbalance between two output ports of the designed PD is presented in Fig. 9. The measured results demonstrated that the difference in phase between two output ports does not exceed 1.2 degrees. The slight difference between simulation and measurement is caused by the SMA connector which was not de-embedded in the measurement.

The measured performances of the proposed two-way PD compared with other reported works are summarized in Tab. 3.

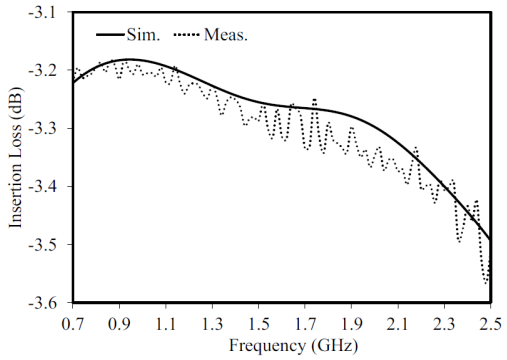

Fig. 7. Simulated (Sim.) and measured (Meas.) insertion loss of the proposed two-way PD.

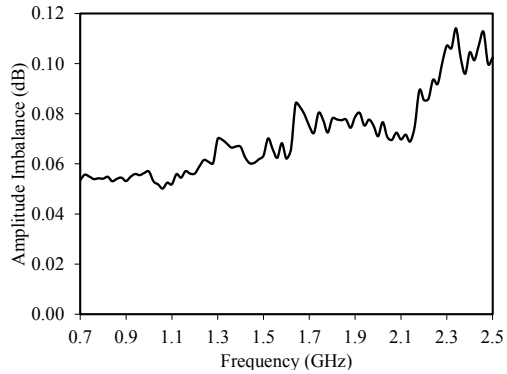

Fig. 8. Measured amplitude imbalance of the proposed two-way PD.

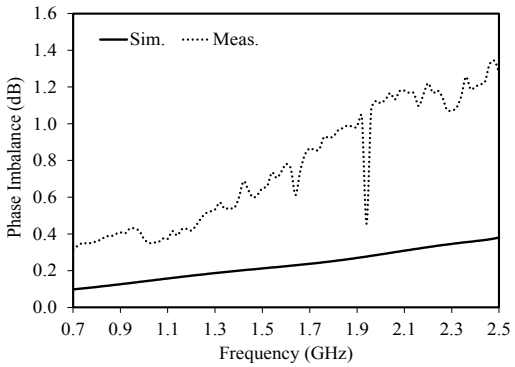

Fig. 9. Simulated and measured phase imbalance between output ports of the designed PD.

Ref.	Material	f_0/FBW (%)	IL (dB)	IS (dB)	Size (cm × cm)
[3]	x	5.5/91	0.2–0.4	> 20	3.9 × 3.5
[4]	x	2.0/48	< 0.4	> 20	8.5 × 5.6
[5]	RO4003C	4.0/50	0.2	> 20	1.2 × 0.2
[7]	RO4003C	0.99/56.6	0.3–0.5	> 23	9.5 × 9.5
This work	RO4003C	1.56/106	0.2–0.5	> 30	5.0 × 5.0

Tab. 3. Comparison of the proposed PD with other PDs.

It is clear that the proposed two-way PD exhibits the highest bandwidth and isolation performance, while still retaining good insertion loss when comparing with the other PDs.

4. Simulation and Measurement of the Eight-way Power Divider

An eight-way PD was then designed to further validate the proposed method after the two-way PD had been successfully designed. The eight-way PD is realized by interconnecting the designed two-way PDs. Figure 10 shows the block diagram of the eight-way PD. It is simply implemented by interconnecting the designed multi-section equal two-way PDs.

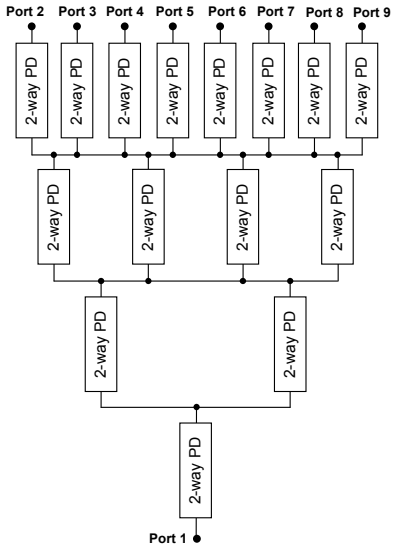

Fig. 10. Block diagram of the proposed eight-way power divider.

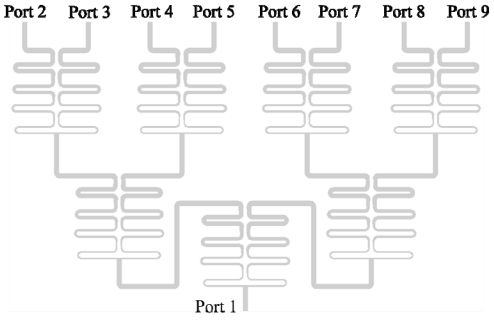

Fig. 11. Layout of the modified eight-way Wilkinson power divider.

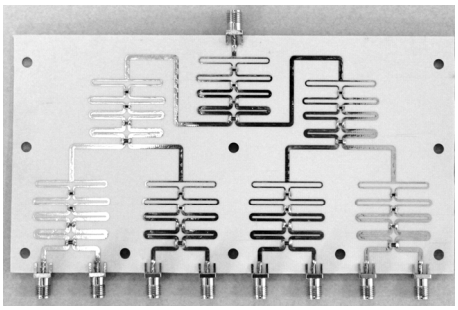

Fig. 12. Photograph of the fabricated prototype of the eight-way Wilkinson power divider.

The layout of the PD is given in Fig. 11 and Fig. 12 shows the fabricated circuit of the prototype. The material used is Rogers RO4003C with a substrate thickness of 22-mil and 1-oz copper thickness. The two-way PD and eight-way PD occupies an area of 5.0 cm × 5.0 cm and 9.0 cm × 16.0 cm, respectively.

4.1 Insertion Loss and Bandwidth

Figure 13 shows the simulated and measured results of the insertion loss of the eight-way PD.

It can be seen from Fig. 13 and Fig. 14 that the simulations agree well with the measurements in the entire frequency range from 0.8 GHz to 2.2 GHz as expected. In this frequency range, the measured insertion loss of the eight-way PD ranges from –10.8 dB to –9.5 dB. This measured low insertion loss in the frequency band of interest well validates the accuracy of the proposed design.

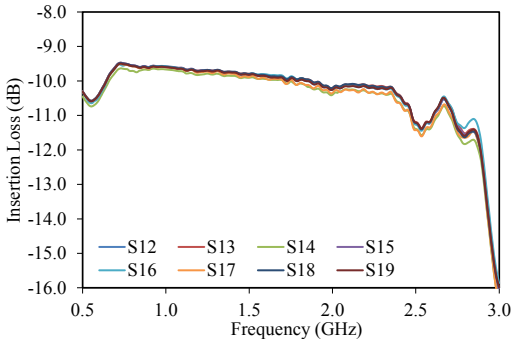

Fig. 13. Simulated insertion loss of the eight-way PD prototype.

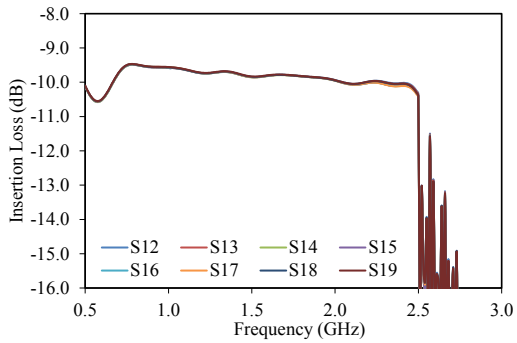

Fig. 14. Measured insertion loss of the eight-way PD prototype.

4.2 Isolation

The eight-way PD has 8 output ports, so it has a total of 28 port pairs. Therefore, the isolation between adjacent ports which have the lowest isolation will be dominated. The simulation and measurement results of the isolation of these port pairs are indicated in Fig. 15 and Fig. 16.

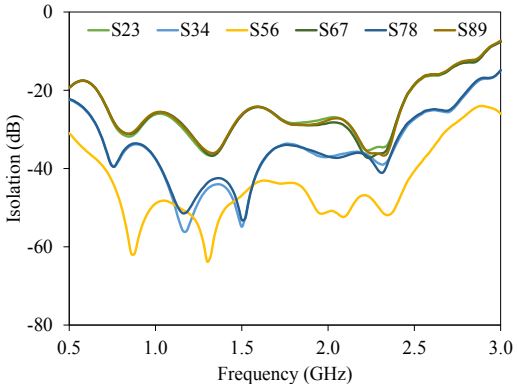

Fig. 15. Simulated isolation between output ports of the eight-way PD.

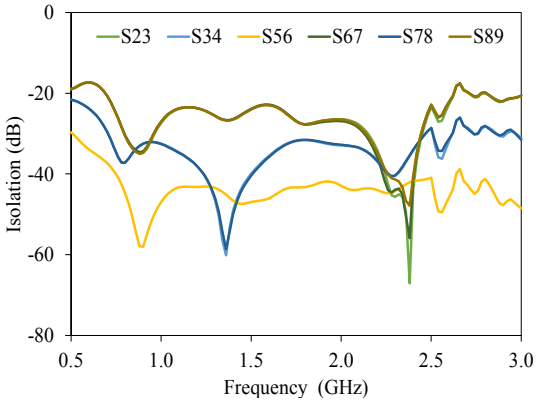

Fig. 16. Measured isolation between output ports of the eight-way PD.

As can be seen from Fig. 15 and Fig. 16, the simulated and measured isolation between adjacent output ports are better than 24 dB over the frequency range from 0.7 to 2.4 GHz.

4.3 Amplitude and Phase Imbalance

The simulated and measured amplitude imbalance between output ports of the eight-way PD are plotted in Fig. 17 and Fig. 18. Good agreements between the simulation and measurement are observed. It is clear that the amplitude imbalances are less than 0.018 dB in the frequency range from 0.8 GHz to 2.2 GHz.

The simulated and measured phase imbalance between the two adjacent output ports is shown in Fig. 19 and Fig. 20.

As can be seen from Fig. 18 and Fig. 19, good agreements between the simulated and measured results are

achieved. It can be seen in Fig. 19 that the differences in phase between the output ports are less than 3 degrees. Finally, a comparison between the proposed eight-way PD and the other works are tabulated in Tab. 4.

From Tab. 4, it can be observed that the proposed PD exhibits a better bandwidth and isolation performance than

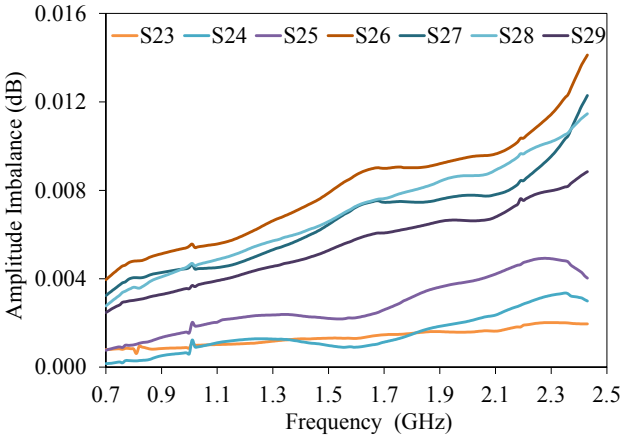

Fig. 17. Simulated amplitude imbalances between output ports of the 8–way PD.

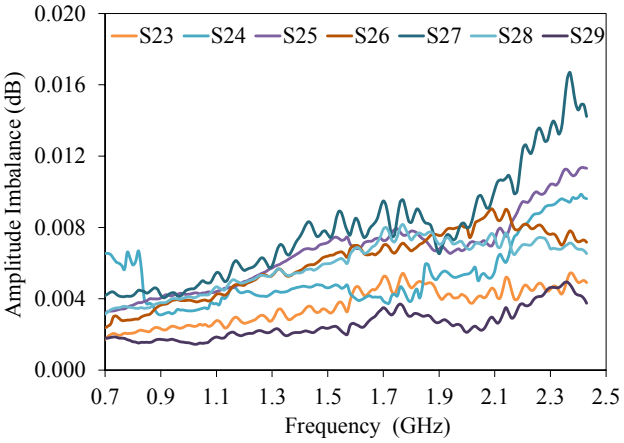

Fig. 18. Measured amplitude imbalances between output ports of the 8–way PD.

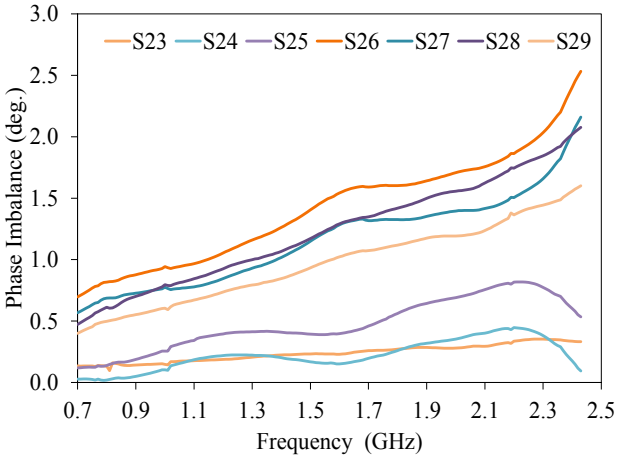

Fig. 19. Simulated phase imbalance between output ports of the 8–way PD.

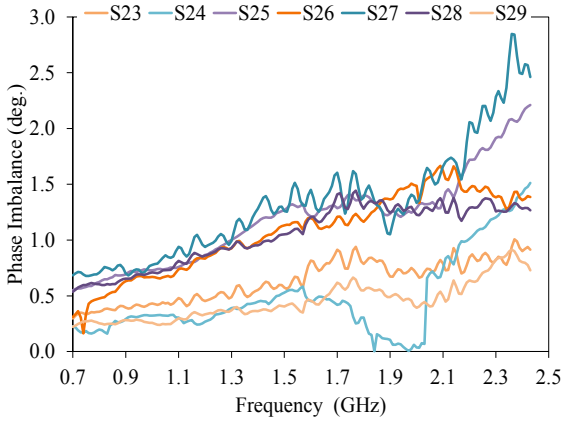

Fig. 20. Measured phase imbalance of the 8–way PD.

Ref.	Material	f_0 (GHz)/ FBW(%)	IL (dB)	IS (dB)	AI (dB)	PI (deg.)	Size (cm × cm)
[13]	RF-35	2.2/36.4	± 0.32	> 20	NI	NI	2.2 × 2.4
[14]	RT 5880	1.38/91	NI	> 15	NI	NI	2.9 × 3.2
[15]	FR4	0.92/44	> 1.1	> 20	NI	NI	11.0 × 11.0
[16]	NI	1.3/77	< 1.5	> 22	< 0.5	< 5	NI
[17]	RO4003C	2.4/13	NI	> 19	<0.16	NI	5.0 × 5.0
This work	RO4003C	1.57/109	0.5–1.8	> 24	<0.02	< 3	9.0 × 16.0

Tab. 4. Comparison with some published eight-way PDs. Here, IL is Insertion Loss; IS is Isolation; AI is Amplitude Imbalance; PI is Phase Imbalance; NI is No Information.

other reported PDs. This superior performance of the proposed PD validates the accuracy of the proposed design method.

5. Conclusions

In this paper, a simple design approach for improving both the bandwidth and isolation of a Wilkinson PD is proposed. The bandwidth was improved by the multi-section impedance transformation based on the TSR method. The isolation was then improved by a separate process via determining the values of the isolation resistors thanks to the investigation process. To validate the proposed approach, a two- and an eight-way PD prototypes were fabricated and tested. The measurement results well matched with those obtained in simulations. In the experiments, the two-way PD delivered a bandwidth of 106%, with an isolation of better than 30 dB. The eight-way PD achieved a FBW of 109%, with an isolation of better than 24 dB, a phase imbalance of less than 3 degrees, and an amplitude imbalance of less than 0.02 dB. Compared with the other works, the proposed PDs exhibited a broader bandwidth and improved isolation, while still retaining good insertion loss and low phase and amplitude imbalance in the operation frequency range.

References

[1] RAUF, A. A., TAHIR, J., RAZA, A., et al. 16 ways X-band Wilkinson power divider for phased array transmitter. In *Proceeding of the 15th International Bhurban Conference on Applied Sciences and Technology*. Islamabad (Pakistan), 2018, p. 835–840. DOI: 10.1109/IBCAST.2018.8312321

[2] WANG, S., CHIANG, M.-J., CHANG, C.-T. A novel CMOS 24-GHz in-phase power divider using synthetic coupled lines. *IEEE Transactions on Components, Packaging and Manufacturing Technology*, 2016, vol. 5, no. 3, p. 398–403. DOI: 10.1109/TCPMT.2015.2401039

[3] PACKIARAJ, D., RAMESH, M., KALGHATGI, A. T. Broadband equal power divider. *Journal of Microwaves, Optoelectronics and Electromagnetic Applications*, 2017, vol. 16, no. 2, p. 363–370. DOI: 10.1590/2179-10742017v16i2757

[4] XU, K., XU, J., LI, D. Wilkinson filtering power divider using coupled lines and T-shaped stub. *Microwave and Optical Technology Letters*, 2019, vol. 61, no. 11, p. 2540–2544. DOI: 10.1002/mop.31914

[5] SINGH, P. K., BASU, S., WANG, Y.-H. Coupled line power divider with compact size and bandpass response. *Electronics Letters,* 2009, vol. 45, no. 17, p. 892–894. DOI: 10.1049/el.2009.1488

[6] LAN, X., CHANG-CHIEN, P., FONG, F., et al. Ultra-wideband power divider using multi-wafer packaging technology. *IEEE Microwave and Wireless Components Letters*, 2011, vol. 21, no. 1, p. 46–48. DOI: 10.1109/LMWC.2010.2091262

[7] CHAO, S.-F., LIN, W.C. Filtering power divider with good isolation performance. *Electronics Letters*, 2014, vol. 50, no. 11, p. 815–817. DOI: 10.1049/el.2014.0171

[8] KAO, J., TSAI, Z., LIN, K., et al. A modified Wilkinson power divider with isolation bandwidth improvement. *IEEE Transactions on Microwave Theory and Techniques*, 2012, vol. 60, no. 9, p. 2768–2780. DOI: 10.1109/TMTT.2012.2206402

[9] LAKRIT, S., MEDKOUR, H., DAS, S., et al. Design and analysis of integrated Wilkinson power divider fed conformal high gain UWB array antenna with band rejection characteristics for WLAN applications. *Journal of Circuits, Systems and Computers*, 2021, vol. 30, no. 8, p. 1–20. DOI: 10.1142/S0218126621501334

[10] DENG, Y., WANG, J., ZHU, L., et al. Filtering power divider with good isolation performance and harmonic suppression. *IEEE Microwave and Wireless Components Letters*, 2016, vol. 26, no. 12, p. 984–986. DOI: 10.1109/LMWC.2016.2623244

[11] POZAR, D. M. *Microwave Engineering*. New York: Wiley, 2012. ISBN: 978-0-470-63155-3

[12] COHN, S. B. A class of broadband three-port TEM-mode hybrids. *IEEE Transactions on Microwave Theory and Techniques*, 1968, vol. 16, no. 2, p. 110–116. DOI: 10.1109/TMTT.1968.1126617

[13] SONG, K., ZHAO, P., CHEN, Y., et al. Compact high-isolation planar eight-way power divider using zero-phase isolation circuit. *IET Microwaves, Antennas & Propagation*, 2020, vol. 14, no. 8, p. 774–778. DOI: 10.1049/iet-map.2019.0788

[14] CHEN, A., ZHUANG, Y., ZHOU, J., et al. Design of a broadband Wilkinson power divider with wide range tunable bandwidths by adding a pair of capacitors. *IEEE Transactions on Circuits and Systems II: Express Briefs*, 2019, vol. 66, no. 4, p. 567–571. DOI: 10.1109/TCSII.2018.2803076

[15] YU, T., LIN, B. S., CHANG, Y. Eight-way radial power splitter including ring shape isolation network. *Electronics Letters*, 2017, vol. 53, no. 24, p. 1587–1589. DOI: 10.1049/el.2017.3486

[16] HONG, Y., KIMBALL, D. F., ASBECK, P. M., et al. Single-ended and differential radial power combiners implemented with a compact broadband probe. *IEEE Transactions on Microwave Theory and Techniques*, 2010, vol. 58, no. 6, p. 1565–1572. DOI: 10.1109/TMTT.2010.2049165

[17] KHAN, A. A., MANDAL, M. K. Miniaturized substrate integrated waveguide (SIW) power dividers. *IEEE Microwave and Wireless Components Letters*, 2016, vol. 26, no. 11, p. 888–890. DOI: 10.1109/LMWC.2016.2615005

About the Authors …

Nguyen Minh GIANG was born in Thai Nguyen, Viet Nam. He received the D.E. degree in Electronics Engineering from Irkutsk National State Technical University, Russia in 2018. He is currently a lecturer at the Le Quy Don Technical University, Hanoi, Vietnam. His research interests include RF design and microwave engineering.

Luong Duy MANH (corresponding author) was born in Son La, Vietnam. He received the B.S. and M.S. degrees in Physics from the Hanoi University of Science (HUS), a member of the Vietnam National University (VNU), Hanoi, Vietnam, in 2005 and 2007, respectively, and the D.E. degree in Electronics Engineering from the University of Electro-Communications (UEC), Tokyo, Japan, in March 2016. He worked at the Graduate School of Engineering Science, Osaka University, Japan as a postdoctoral researcher from April 2016 to June 2017. He is currently a lecturer at the Le Quy Don Technical University, Hanoi, Vietnam. His research interests include development of microwave semiconductor devices and circuits and terahertz (THz) integrated systems for wireless communication applications based on resonant tunneling diodes (RTDs) and photonic crystals.